

Flare Response versus Disease Progression in Patients with Non-small Cell Lung Cancer

Khalsa Al-Nabhani^{1*}, Rizwan Syed¹, Athar Haroon¹, Omar Almukhailed¹, Jamshed Bomanji¹

1. Institute of Nuclear Medicine, University College London Hospitals, London, UK

* **Correspondence:** Khalsa Al-Nabhani, Institute of Nuclear Medicine, University College London Hospitals, T5, 235 Euston Road, NW1 2BU, London, UK
(✉ alnabhani5@hotmail.com)

Radiology Case. 2012 Nov; 6(11):34-42 :: DOI: 10.3941/jrcr.v6i11.1109

ABSTRACT

We present a case report of a patient with metastatic non-small cell lung cancer (NSCLC) who had a series of fluorine-18 fluorodeoxyglucose positron emission tomography/computed tomography (18F-FDG PET/CT) scans for assessment of response to treatment. A restaging 18F-FDG PET/CT scan after six cycles showed increased FDG activity in the bone lesions with reduced activity in the lung and liver lesions. The increased bone activity was considered to be due to flare phenomenon rather than metastasis. A short interval follow up scan after 1 month was advised to confirm this interpretation but this repeat scan showed disease relapse. Although the flare phenomenon does exist, caution should be exercised in attributing increased tracer uptake in the lesions in patients with adenocarcinoma of lung and especially those who have received erlotinib during the course of their treatment. Distinguishing the 'flare phenomenon' and 'disease progression' is at times difficult but is important since misdiagnosis may result in an unnecessary delay in patient management.

CASE REPORT

CASE REPORT

A 59-year-old male presented to his general practitioner with hoarseness of voice, reduced appetite and right hip and left shoulder pain. In addition, he complained of mild exertional dyspnoea but had no other significant chest symptoms. Chest radiography showed a mass in the upper lobe of the left lung and the baseline CT scan demonstrated a 3 cm spiculated mass and satellite nodules in the same lobe. Multiple metastatic lesions were found in the liver. In addition mediastinal and left hilar lymph node metastases were noted [Figures 1, 2]. Subsequent magnetic resonance imaging (MRI) of the spine confirmed bone metastases within the spine, sacrum and proximal femora [Figure 3].

The baseline 18F-FDG PET/CT scan showed intense uptake in the 3 cm mass in the upper lobe of the left lung, mediastinal nodes, left hilar nodes and multiple liver and bone lesions [Figure 4]. Chemotherapy (cisplatin and pemetrexed) and palliative radiotherapy were commenced after biopsy of

the left scapular mass which showed an adenocarcinoma that demonstrated positive immuno-staining for CK7 (cytokeratin 7) and TTF1 (thyroid transcription factor-1) compatible with primary lung carcinoma [Figure 5].

A follow-up 18F-FDG PET/CT scan after two cycles of chemotherapy showed a significant reduction in tracer avidity with mild uptake in the left upper lobe lung mass (maximum standardised uptake value (SUVmax) 3.2; previously 20.4) and multiple bone lesions (SUVmax 3.6; previously 8.4). No uptake was seen in the mediastinal nodes, left hilar nodes or liver lesions.

After four cycles, 18F-FDG PET/CT scan demonstrated that uptake in the majority of the skeletal lesions and the chest lesions was unchanged, and the patient was therefore classified as having stable disease at this stage [Figure 6a]. Erlotinib [epidermal growth factor receptor (EGFR) tyrosine kinase inhibitor] was added to the treatment regimen and a restaging 18F-FDG PET/CT was performed after six cycles of treatment

which showed no significant tracer uptake in the lung nodules, mediastinal nodes or liver lesions. However, FDG uptake in the bone lesions showed a further increase in metabolic activity of about 51.5% (SUVmax 6.8 previously 3.5) [Figure 6 b]. Although the bone lesions now appeared sclerotic on CT, the pattern of FDG uptake was very unusual, with no uptake in the rest of the metastatic lesions. At this stage the bone lesion uptake was thought to represent a 'flare response phenomenon' rather than 'disease progression' [Figure 6 b]. A short-interval follow-up scan was advised, and repeat 18F-FDG PET/CT after a month showed evidence of disease relapse in the chest (mediastinal lymph nodes) and liver, with increased uptake in the bone lesions [Figure 7]. This confirmed disease progression within the bone lesions rather than a 'flare response' as previously thought.

DISCUSSION

Lung cancer is the most common cancer in the world and accounts for 13% [1] of all new cases of cancer. NSCLC in turn accounts for 75-85% of all lung cancers (M:F ratio, 1.3:1). Tobacco smoking is one of the major risk factors for lung cancer and is considered the cause of death in as many as 90% of patients. The 5-year relative survival rate and the choice of treatment depend on the tumour stage at diagnosis [1,2,3] [Table 1].

Various modalities are used to diagnose lung cancer and one should be aware of the differential diagnoses such as metastasis and benign lesions which may mimic the disease [Table 2].

18F-FDG PET/CT has largely replaced technetium-99m methylene diphosphonate (99mTc-MDP) for the evaluation of suspected bone metastases. It is more sensitive and more specific than other currently available modalities for this purpose [4,5,6]. 18F-FDG PET/CT delineates the exact location of uptake in both osseous and non-osseous lesions, obviating the need for additional imaging. Patients with NSCLC have a 30%-40% likelihood of developing bone metastases [7]. The bony lesions in NSCLC are predominantly osteolytic but are occasionally osteoblastic (around 9%) [8]. In particular, it has been documented that adenocarcinoma of the lung may have osteoblastic bone deposits [8]. In addition, patients receiving erlotinib for NSCLC may develop osteoblastic bone lesions secondary to treatment response, and care should be exercised in recognising these features. As would be expected, response to treatment is reflected by a variable reduction in FDG uptake in almost all lesions. In some cases, however, there is increased uptake in bone lesions, seen both on 99mTc-MDP bone scan and on 18F-FDG PET/CT. This is attributed to the flare response phenomenon and is explained by increased osteoblastic activity at the site of metastatic bone lesions owing to the rapid repair; it accordingly represents response to treatment rather than disease progression. The flare response phenomenon has been described in the medical literature with regard to bone metastases secondary to breast and prostate cancer, as well as NSCLC [9-12].

18F-FDG PET/CT assesses the response to treatment by evaluating the reduction in metabolic activity in the primary tumour and metastases. In the reported case, there was a reduction in metabolic activity in the primary tumour and metastatic nodal and liver lesions during the course of the treatment, but increased metabolic activity in the bone lesions, i.e. FDG uptake in the bone metastases did not diminish, as would be expected. Technical errors were excluded to ensure that the increase in FDG activity was genuine, and the patient was erroneously considered to have the above-mentioned flare response following chemotherapy and radiotherapy. However, since no reliable markers can differentiate the flare phenomenon from disease progression, a short follow-up scan together with careful CT correlation should be performed in order to confirm or exclude disease relapse, and this approach was adopted in the reported case.

Awareness of this issue of disease progression versus flare phenomenon is especially important in patients with adenocarcinoma of lung and those who have received erlotinib during their course of treatment, such as our patient. This is because there is a tendency for NSCLC patients who have an EGFR gene mutation and are on erlotinib to show an osteoblastic flare response [2,3]. Erlotinib acts by inhibiting EGFR and hence induces osteoblastic proliferation and prevents osteoclastic activation [2, 3]. This important potential pitfall needs to be borne in mind by clinicians when interpreting increased FDG uptake.

TEACHING POINT

Awareness of the difficulty in distinguishing between the flare phenomenon and disease progression is important in enabling clinicians to avoid premature cessation of treatment or unnecessary changes in the treatment course, especially in patients with NSCLC (adenocarcinoma) who have been treated with erlotinib. Definitive diagnosis is possible only after short-interval follow-up with 18F-FDG PET/CT.

REFERENCES

1. Bordoni A, Bongioivanni M, Mazzucchelli L, Spitale A. Impact of histopathological diagnosis with ancillary immunohistochemical studies on lung cancer subtypes incidence and survival: a population-based study. *J Cancer Epidemiol.* 2011;2011:275758. Epub 2011 Dec 29. PMID: 22253626
2. Lind JS, Postmus PE, Smit EF. Osteoblastic bone lesions developing during treatment with erlotinib indicate major response in patients with non-small cell lung cancer: a brief report. *J Thorac Oncol.* 2010 Apr;5(4):554-7. PubMed PMID: 20357621.
3. Wang M, Zhao J, Zhang LM, Li H, Yu JP, Ren XB, Wang CL. Combined Erlotinib and Cetuximab overcome the acquired resistance to epidermal growth factor receptors

tyrosine kinase inhibitor in non-small-cell lung cancer. *J Cancer Res Clin Oncol.* 2012 Jul 22. PMID:22821179

4. Chang MC, Chen JH, Liang JA, Lin CC, Yang KT, Cheng KY, Yeh JJ, Kao CH. Meta-analysis: comparison of F-18 fluorodeoxyglucose-positron emission tomography and bone scintigraphy in the detection of bone metastasis in patients with lung cancer. *Acad Radiol.* 2012 Mar;19(3):349-57. PMID: 22173321
5. Hoh CK, Schiepers C, Seltzer MA, Gambhir SS, Silverman DH, Czernin J, Maddahi J, Phelps ME. PET in oncology: will it replace the other modalities? *Semin Nucl Med.* 1997 Apr;27(2):94-106. Review. PubMed PMID: 9144854.
6. Song JW, Oh YM, Shim TS, Kim WS, Ryu JS, Choi CM. Efficacy comparison between (18)F-FDG PET/CT and bone scintigraphy in detecting bony metastases of non-small-cell lung cancer. *Lung Cancer.* 2009 Sep;65(3):333-8. PubMed PMID: 19144446
3. Cook GJ, Fogelman I. The role of positron emission tomography in the management of bone metastases. *Cancer.* 2000 Jun 15;88(12 Suppl):2927-33. Review. PubMed PMID: 10898336.
8. Napoli LD, Hansen HH, Muggia FM, Twigg HL. The incidence of osseous involvement in lung cancer, with special reference to the development of osteoblastic changes. *Radiology.* 1973 Jul;108(1):17-21. PubMed PMID: 4350792.
9. Coleman RE, Mashiter G, Whitaker KB, Moss DW, Rubens RD, Fogelman I. Bone scan flare predicts successful systemic therapy for bone metastases. *J Nucl Med.* 1988 Aug;29(8):1354-9. PubMed PMID: 3261330.
10. Vogel CL, Schoenfelder J, Shemano I, Hayes DF, Gams RA. Worsening bone scan in the evaluation of antitumor response during hormonal therapy of breast cancer. *J Clin Oncol.* 1995 May;13(5):1123-8. PubMed PMID: 7537797.
11. Schneider JA, Divgi CR, Scott AM, Macapinlac HA, Seidman AD, Goldsmith SJ, Larson SM. Flare on bone scintigraphy following Taxol chemotherapy for metastatic breast cancer. *J Nucl Med.* 1994 Nov;35(11):1748-52. PubMed PMID: 7525900.
12. Janicek MJ, Hayes DF, Kaplan WD. Healing flare in skeletal metastases from breast cancer. *Radiology.* 1994 Jul;192(1):201-4. PubMed PMID: 8208938.

FIGURES

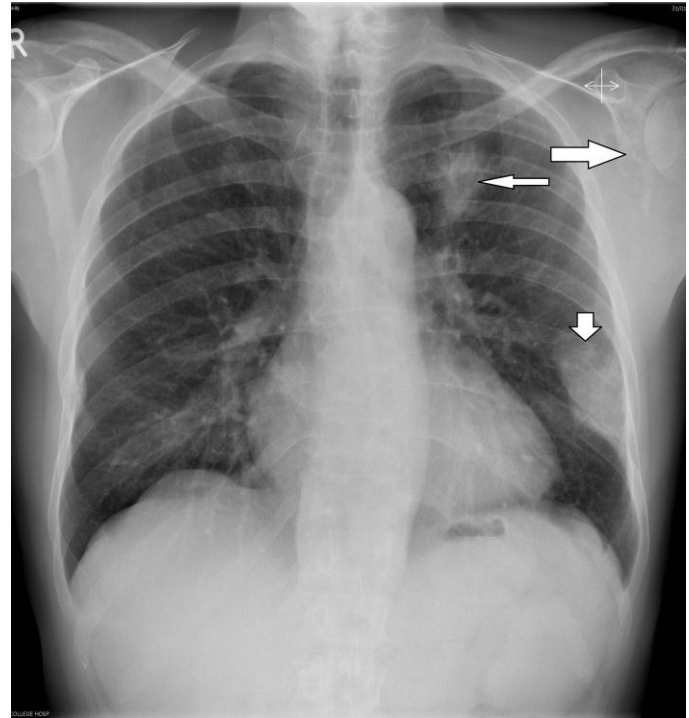


Figure 1: A 59 year old male with metastatic non small cell lung cancer. Plain chest radiograph, posterior-anterior view shows an ill-defined spiculated opacity in the left upper zone (thin arrow). In addition, there is a pathological fracture of the left 7th rib and an expansile lytic lesion with soft tissue component involving the left 8th rib posteriorly (thick arrow). A further suspicious osteolytic lesion is seen in the left scapula (long thick arrow).

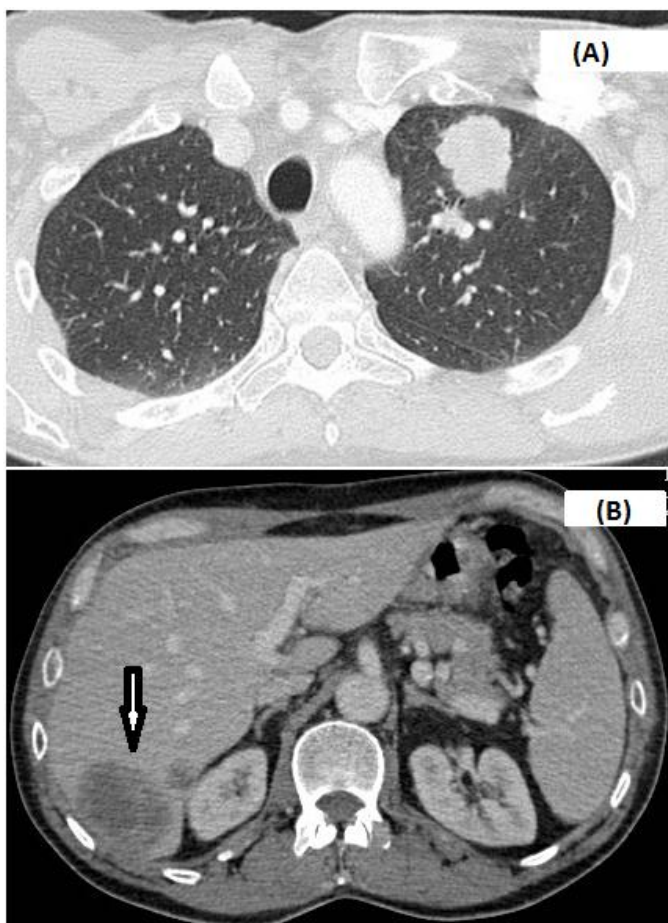


Figure 2: A 59 year old male patient with metastatic non small cell lung cancer. A) Axial CT section (lung window) from a post contrast-enhanced CT scan of the chest and abdomen, shows a 3cm spiculated mass in the upper lobe of the left lung anteriorly with an adjacent small satellite nodule. B) Abdomen image section obtained at the level of the renal hilum from the same post contrast CT chest and abdomen. There are two hypodense lesions in the right liver lobe (segment 6) which show mild contrast enhancement (arrow). (Protocol: 120 kV, 250 mAs, slice thickness 2.5 mm (chest and abdomen), iohexol (omnipaque), 100 ml).

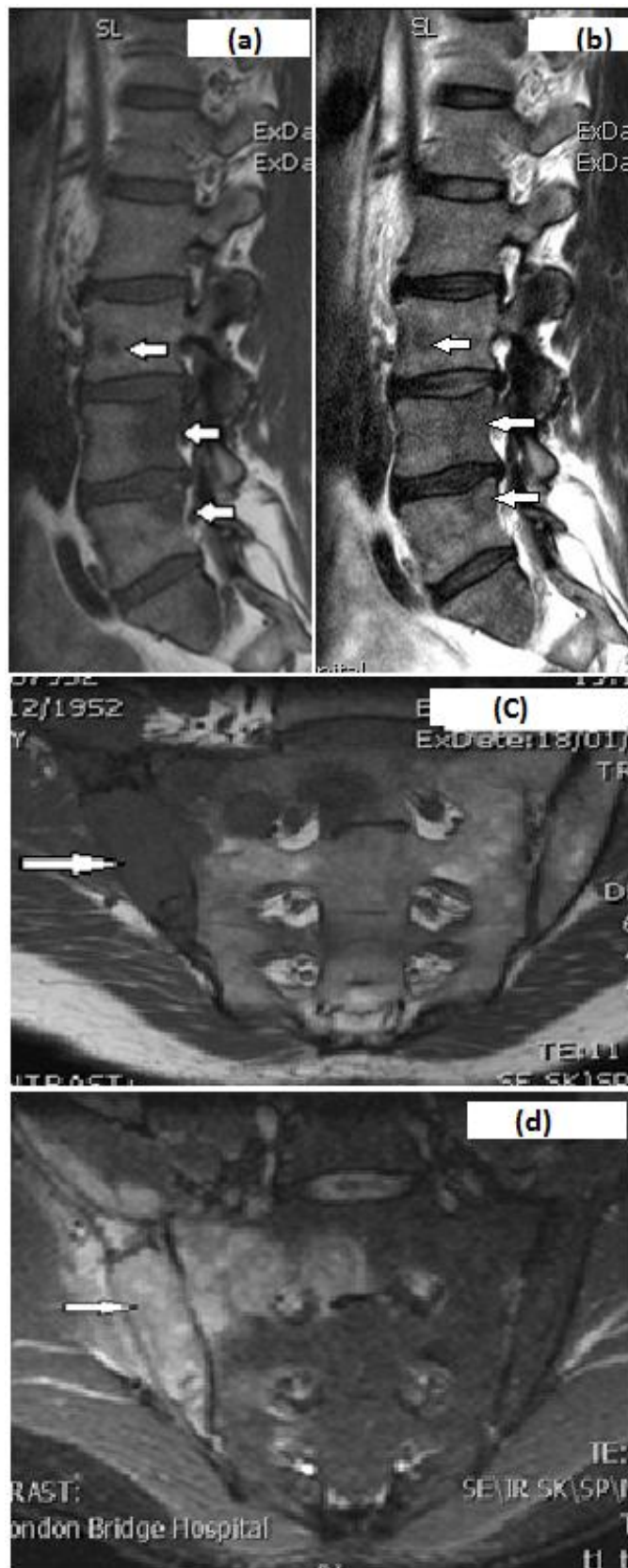


Figure 3 (right): A 59 year old male patient with metastatic non small cell lung cancer. a, b) Sagittal T1W and T2W images show multiple hypointense on T1W and isointense on T2W at L3, L4 and L5 vertebral bodies (arrows). c) Coronal T1W pre-contrast image shows an expansile hypointense lesion involving the right iliac bone (thin arrow) with extension into the adjacent right sacrum. d) Coronal T1W (STIR) post contrast image shows intense enhancement involving the right iliac crest and sacrum with extension into the right gluteal and right piriformis muscles. (Protocol: Siemens, 1.5 Tesla magnet, sagittal T1 (TR/TE: 516/11) and T2 (3000/87), coronal T1 pre-contrast and T1 STIR post contrast (TR/TE 3800/30), 3 mm slice thickness, 10 ml gadolinium).

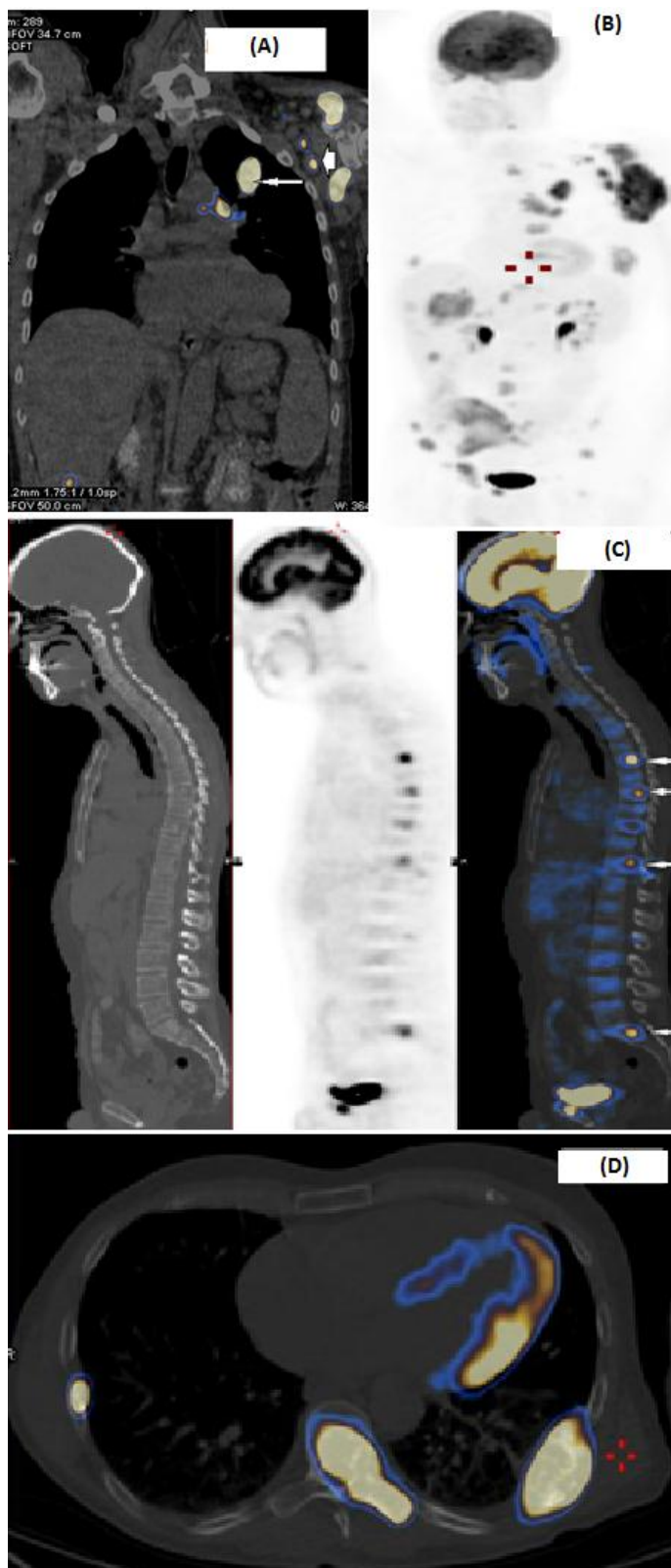


Figure 4: 18F-FDG PET/CT, baseline study, (Maximum intensity projection and Coronal, Sagittal and Axial fusion images). A 59 year old male with metastatic non small cell lung cancer. A) Coronal fused image from a baseline 18F-FDG PET/CT performed for staging of the disease demonstrated increased 18F-FDG uptake in the left upper lobe mass (SUVmax 20.5, thin arrow), left hilar, mediastinal, multiple axillary lymph nodes (thick arrow) and the left scapular bony lesion. B) Whole -body MIP images from the same scan shows abnormal 18F-FDG uptake in the left upper lobe, hilar, mediastinal, left supraclavicular and left axillary lymph nodes, left scapula, multiple liver lesions and multiple spinal lesions. C) Sagittal CT bone window, MIP and fused images show multiple lytic lesions in the thoracic spine and sacrum and pubic bone with increased 18F-FDG uptake (thin arrows). D) Axial fused image of the chest at the level of the left ventricle, demonstrating lytic expansile bilateral rib lesions (left 8th and right 7th ribs) and a lesion of the T9 vertebral body extending to the left pedicle and transverse process. These lesions show increased 18F-FDG activity.

mediastinal, left supraclavicular and left axillary lymph nodes, left scapula, multiple liver lesions and multiple spinal lesions. C) Sagittal CT bone window, MIP and fused images show multiple lytic lesions in the thoracic spine and sacrum and pubic bone with increased 18F-FDG uptake (thin arrows). D) Axial fused image of the chest at the level of the left ventricle, demonstrating lytic expansile bilateral rib lesions (left 8th and right 7th ribs) and a lesion of the T9 vertebral body extending to the left pedicle and transverse process. These lesions show increased 18F-FDG activity. (Protocol: Whole body MIP and fused image from 18F-FDG PET/CT, 120 kVp, 2.5 mm slice thickness, 366 MBq of 18F-FDG was injected and imaging was performed at 65 min).

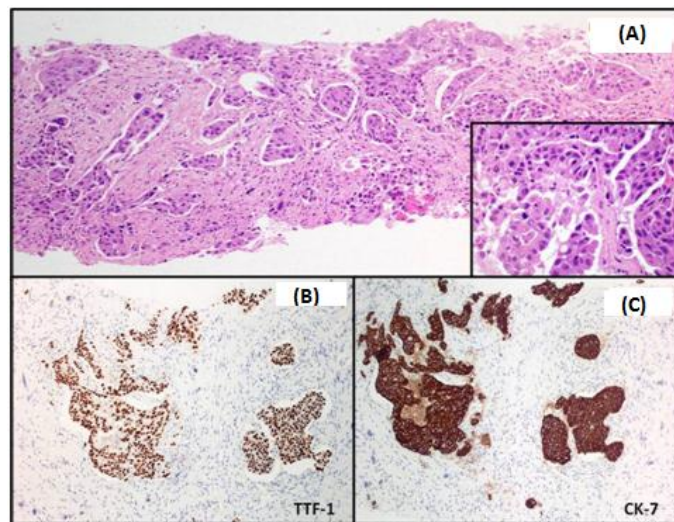


Figure 5: A 59 year old male with metastatic non small cell lung cancer. 5A) Magnified photomicrograph of Hematoxylin and Eosin (H&E) core biopsy specimen of the soft tissue infiltrating the left scapula shows fibrous connective tissue and skeletal muscle extensively infiltrated by a metastatic poorly differentiated adenocarcinoma. (Magnification 10x for main image and 40X for the smaller image at the corner.) 5B, 5C) Images (20x magnification) of the same specimen with Immunohistochemistry shows the tumour cells to be diffusely and strongly positive for TTF1 and CK7 respectively. The morphological features and immunoprofile are in keeping with a metastatic primary lung adenocarcinoma.

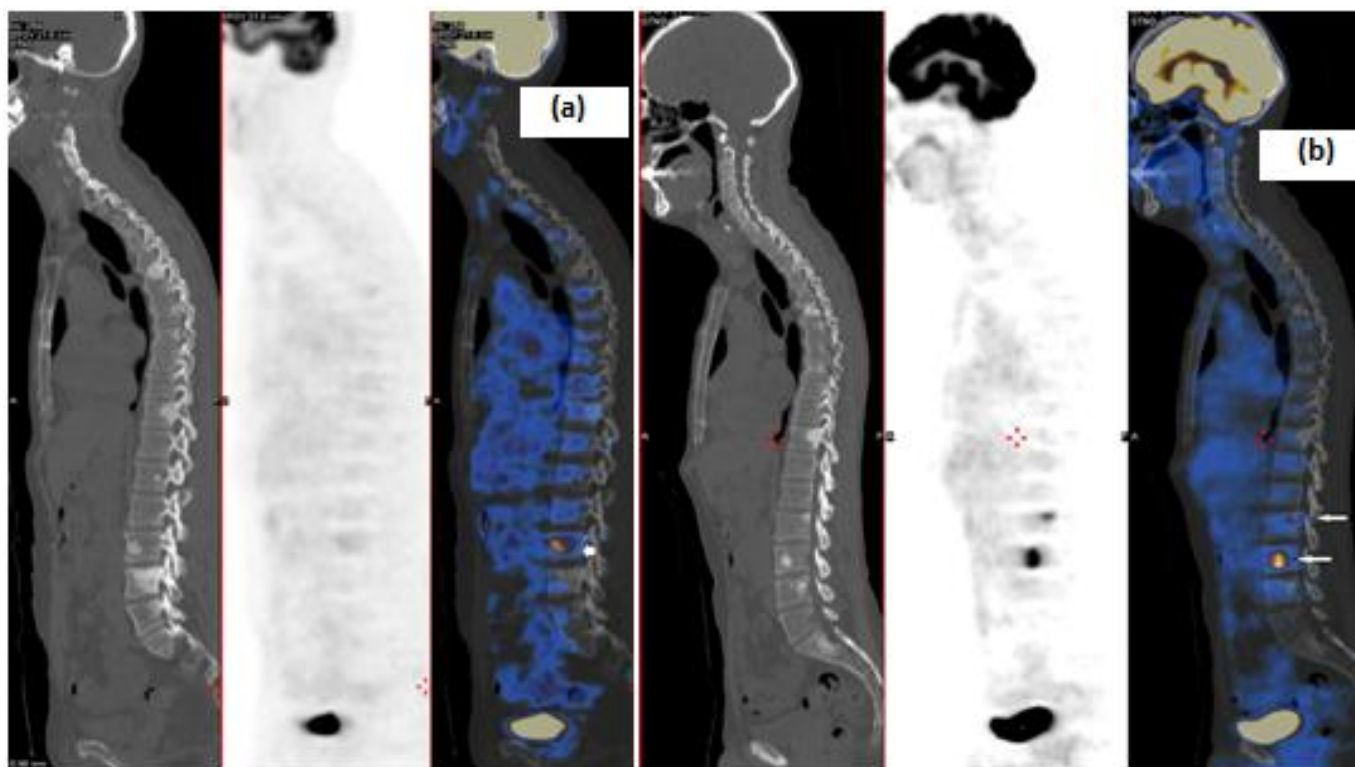


Figure 6: 18F-FDG PET/CT post 4th and 6th cycle of chemotherapy (CT, MIP and fused sagittal images). A 59 year old male with metastatic non small cell lung cancer. a) CT, MIP and fused sagittal images obtained from an 18F -FDG PET/CT follow-up scan after the 4th cycle of chemotherapy which showed multiple sclerotic bony lesions along the entire spine at T5, T11, L1, L3, L4 and L5 vertebrae. L2, L3 vertebral body lesions show mild 18F-FDG activity (L3; SUV max 3.5) (thin arrow) whereas the other lesions are non 18F-FDG avid. b) CT, MIP and fusion Sagittal images obtained from an 18F-FDG PET/CT follow-up scan after the 6th cycle of chemotherapy which show multiple sclerotic bony lesions seen at T5, T6, T11, L2, L3, L4, L5 and S1 vertebrae. L2 and L3 vertebral body lesions (arrow) show increased 18F-FDG activity (L3; SUV max 6.8, previously 3.5). (Protocol: Whole-body MIP , CT and fused images from 18F-FDG PET/CT, 120 kVp, 2.5 mm slice thickness, 410 MBq and 446 MBq of 18F-FDG was injected respectively, and imaging was performed at 60 min).

www.RadiologyCases.com

Journal of Radiology Case Reports

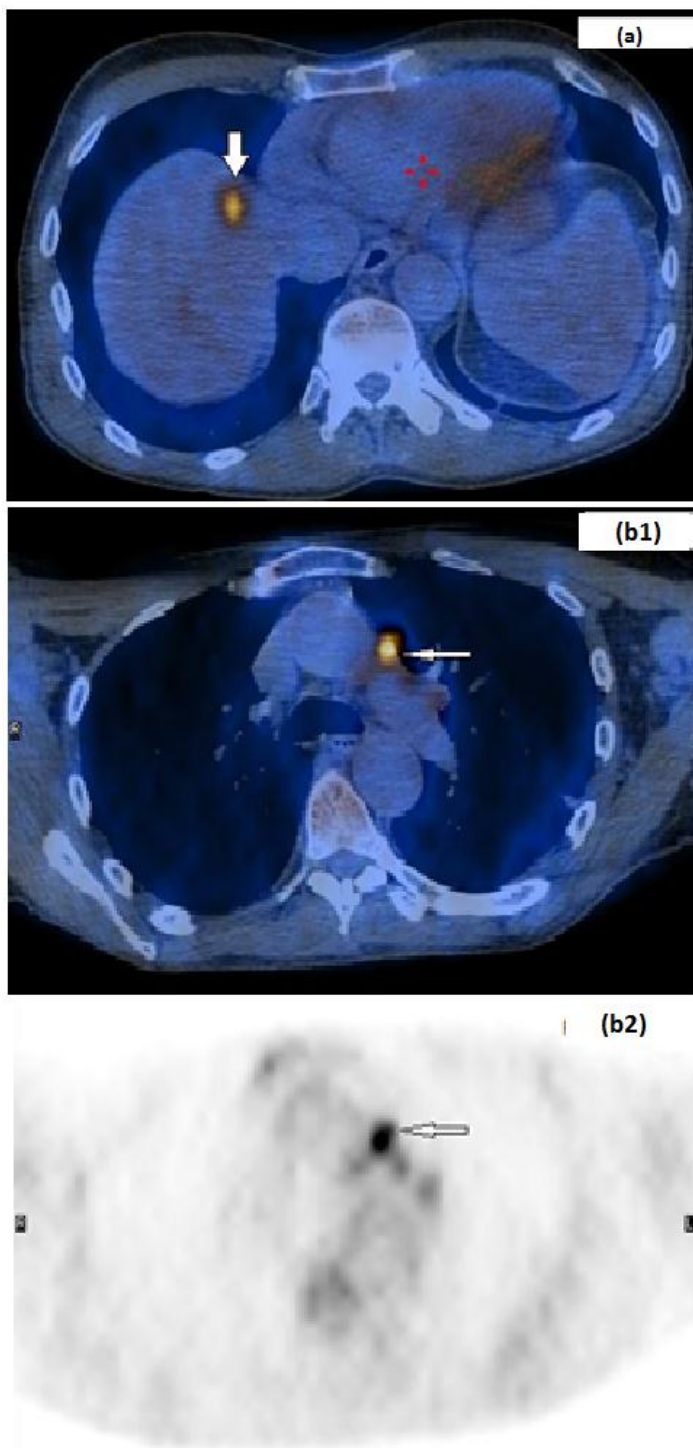


Figure 7: Follow-up 18F-FDG PET/CT scan after 1 month (CT/PET fused axial images, PET axial image). A 59 year old male with Non small cell lung cancer with metastasis. a) CT/PET fused axial images from whole-body 18F-FDG PET/CT scan obtained after 1 month of the scan labelling the patient with bone flare phenomenon. There is a 1 cm FDG avid hypodense liver lesion (thick arrow). b1, b2) CT/PET fused axial images and axial PET image from 18F-FDG PET/CT images obtained from the same scan show 18F-FDG avid soft tissue density in the AP window (thin arrow) which represents a metastatic lymph node. (Protocol: axial fused and axial PET images from 18F-FDG PET/CT scan, 120 kVp, 2.5 mm slice thickness, 422 MBq of 18F-FDG was injected and imaging was performed at 60 min).

Aetiology	Environmental and occupational factors and an individual's susceptibility to these agents are thought to contribute to risk of developing lung cancer.
Incidence	Lung cancer is the most common cancer in the world with 1.61 million new cases diagnosed every year. 13% of all new cases of cancer are lung cancers. NSCLC accounts for approximately 75-85% of all lung cancers.
Gender ratio	Male to female ratio is 1.3:1.
Age predilection	Most cases (87%) occur in people over the age of 60.
Risk factors	Smoking (78% in men, 90% in women), asbestos exposure, radon exposure, halogen ether exposure, chronic interstitial pneumonitis, inorganic arsenic exposure, radioisotope exposure, ionising radiation, atmospheric pollution, chromium exposure, nickel exposure, vinyl chloride.
Treatment	The treatment options depend on the stage of the cancer. For example, in patients with stage I or II NSCLC the treatment of choice is surgery. Radiation is often prescribed for patients with stage III disease or those with stage I or II disease in whom surgery is not performed. Chemotherapy provides only modest survival benefits (1–2 months) in disseminated NSCLC.
Prognosis	Stage I and II cancers have the highest survival and cure rates (5-year survival rate in stage I is 60-80%, and in stage II, 25-50%). Stage III tumours can be cured in some cases (5-year survival rate for stage IIIA is 10-40% and for stage IIIB, less than 5%). Patients with stage IV cancer that has returned are almost never cured (5-year survival rate is less than 5%); the goals of therapy are to extend and improve their quality of life.
Findings on imaging	
Radiography	Used for screening. Variable findings but the most common are: bronchial stenosis, regional hyperlucency, hilar mass, solitary pulmonary nodule and non-resolving pneumonia.
CT	Used for evaluation of suspicious CXR findings and for staging of disease. Helps to differentiate between benign and malignant lesions based on lesion morphology.
MRI	Used for evaluation of local invasion and detection of hilar lymphadenopathy.
Nucl. Med.	FDG PET scan has been used to differentiate benign from malignant pulmonary nodules, for staging of disease and for evaluation of response to treatment.

Table 1: Summary table of key factors for non-small cell lung cancer.

Diagnosis	X-Ray	CT	FDG PET/CT	Gallium-68 DOTATATE
Malignant tumours				
<i>Primary malignancy (NSCLC)</i>	Peripheral lung opacity/ consolidation, hilar enlargement,	Lung mass, lymphadenopathy, pleural effusion, secondaries.	Increased FDG uptake in the lung lesion and metastatic sites.	Negative
<i>Metastasis</i>	One/ multiple nodules of variable size and possible bone metastasis.	One/multiple nodules of variable size, irregular, often in periphery of lower lung zones.	Increased FDG uptake in nodules and at primary site	Negative
Benign nodules				
<i>Arteriovenous malformation</i>	Round/ oval uniform mass with adjacent linear opacity (feeding vessel)	Enhancing lesion with feeding vessels.	No FDG uptake	Negative
<i>Hamartoma</i>	Rounded, +/- popcorn calcification	Lung nodule with calcification and fatty component	No FDG uptake	Negative
<i>Pneumonia</i>	Patchy consolidation or rounded opacity, +/- pleural effusion.	Patchy consolidation with air bronchogram, lymphadenopathy, pleural effusions.	Variable FDG uptake	+/- Low uptake
<i>Carcinoid</i>	Rounded central opacity, +/- calcification.	Rounded central/ endobronchial opacity, +/- calcification.	No or low FDG uptake	Positive

Table 2: Differential table for non-small lung cancer

ABBREVIATIONS

18F-FDG PET/CT = Fluorine-18 fluorodeoxy glucose Positron emission tomography/ Computed tomography
 99m Tc MDP = 99m Technetium methylene diphosphonate
 CK 7 = Cytokeratin 7
 CT = Computed tomography
 EGFR = Epidermal Growth Factor Receptor
 NSCLC = Non-small cell lung cancer
 MIP = Maximum intensity projection
 MRI = Magnetic resonance imaging
 SUV max = Standard uptake value, maximum
 TTF1 - Thyroid transcription factor-1

KEYWORDS

Flare phenomena; non-small cell lung cancer; NSCLC; 18F-FDG PET/CT; erlotinib; disease progression

ACKNOWLEDGEMENTS

For Dr. Mary Falzon (Consultant Histo/Cytopathologist, University College Hospital, UCLH) for providing us with the histopathology images.

Online access

This publication is online available at:
www.radiologycases.com/index.php/radiologycases/article/view/1109

Peer discussion

Discuss this manuscript in our protected discussion forum at:
www.radiopolis.com/forums/JRCR

Interactivity

This publication is available as an interactive article with scroll, window/level, magnify and more features.
 Available online at www.RadiologyCases.com

Published by EduRad



www.EduRad.org